

BUBBLE FORMATION AT TWO ADJACENT SUBMERGED ORIFICES IN INVISCID FLUIDS

Bashir H Arebi and W. Dempster *

Department of Nuclear Engineering,
Al-Fateh University, Tripoli, Libya
E-mail; Arebi_bashir@yahoo.co.uk

*Strathclyde University, Glasgow, U.K.
William.dempster@strath.ac.uk

المخلص

في هذه الورقة تم تطوير نموذج رياضي لدراسة نمو وانفصال فقائيع الغاز أو البخار المتكونة عند فتحتين متجاورتين مغمورتين في مائع غير لزج النموذج. الرياضي عامل الفقاعتين الناميتين كأنهما حجمين تحكميين يتسعان ويتحركان عموديا على خط المركز فوق جدار صلب. حركة الفقائيع وجدت كنتيجة تأثير محصلة القوة على الفقاعة، والتي تشمل قوى الشد السطحي والطفو والزخم للغاز أو البخار والقصور الذاتي للسائل الذي تم إيجاده بافتراض السائل غير لزج وغير دوراني. النموذج تم دمج مع معادلات الطاقة والكتلة لدراسة فقائيع بخار الماء المتكونة عند الفتحات نتيجة حقن البخار المشبع إلى داخل سائل الماء المضغوط (تحت التشبع). النموذج الرياضي تم مقارنته بنتائج تجريبية متوفرة في مرجع سابق، والتي تتعلق بنمو وانفصال فقائيع بخار الماء المشبع المتدفقة بمعدل كتلة ثابت (1.2 – 4 جرام / دقيقة) خلال فتحتين متجاورتين قطر كل منهما 1 مم ومغمورتين في ماء تحت التشبع (3.5 – 35 م^o) وعند ضغط مطلق 2 و 3 بار. وقد أشارت المقارنة إلى نجاح النموذج الرياضي في محاكاة نمو وانفصال فقائيع البخار المتكونة ضمن شروط الدراسة.

ABSTRACT

A theoretical model has been developed as an extension of single orifice bubble formation to investigate the growth and detachment of vapor/ gas bubbles formed at two adjacent submerged orifices in inviscid fluids. The mathematical model treats the two bubbles as an expanding control volume moving to the line of centers above a wall. The movement of the bubbles is obtained by application of force balance acting on the bubble and accounts for surface tension, buoyancy, steam momentum and liquid inertia effects. The liquid inertia effects are determined by applying inviscid and irrotational flow assumptions to allow potential flow theory to calculate the liquid velocity field which then allows the pressure distribution to be calculated. The model is extended to include the mass and energy equations to model the steam bubble formation in sub-cooled water. The theoretical results are compared with the available experimental data of bubble formation during constant mass flow steam bubble formation at two submerged upward facing orifices in sub-cooled water. The model was validated by available experimental data for the growth and detachment processes of two adjacent 1 mm orifices at system pressures of 2 and 3 bars, flow rates of 1.2-4 g/min at sub-cooling of 3.5-35 °C. The comparisons of theory and experiments indicate that the model successfully predicts the bubbles growth and detachment for the range of conditions studied.

KEYWORDS: Bubble formation and detachment; Multiple orifices; Submerged orifices.

INTRODUCTION

Despite the numerous theoretical and experimental investigations of bubble formation, the mechanisms of bubble growth and detachment at submerged orifices remain far from being fully understood. Previous experimental and theoretical studies have concentrated on the formation of a gas bubble at a single orifice and very few studies have addressed the case of bubble formation at multiple orifices leading to a dearth of information on how the growing bubbles interact at adjacent orifices in bubble columns.

A little has been done on vapour bubble formation at a submerged orifice with transfer phenomena at the bubble wall, like a steam bubble in sub-cooled water. Arebi B. H. and Dempster W [3], Simpson et al [5] and Cho et al [6] studied the formation of steam bubbles at an orifice submerged in sub-cooled water both theoretically and experimentally. The work was limited to the formation of steam bubbles at a single orifice without the influence of bubbles formed at neighbouring orifices.

Very few studies have carried out the case of multiple orifices as extension of single orifice bubbling formation. Most of the studies concerning of multiple bubbling were experimental. Ruzicka et al [8, 9] investigated experimentally gas bubble formation at two orifices and identified two typical modes of bubbling; the synchronous and the asynchronous and concluded that the spacing between orifices plays a key role of mechanism's of bubbling interactions. Shuki and Reginald [10] investigated gas bubble formation at two and multiple orifices and identified three modes of bubbling regimes at multiple orifices depending on the gas flow rates and orifices spacing which is affect bubbling synchronicity, frequency and bubble sizes. Pereira [11] found experimentally that the size, frequency and formation process of bubbles formed at a multiple orifices is influenced by the distance between the orifices as it plays a critical role on the coalescence process of bubbles growing at neighbouring orifices. Dempster W. and Arebi B. [2] investigated a steam bubble formation one and two orifices submerged in subcooled water experimentally and conclude for constant steam flow rate that the neighbouring orifice affect the formation frequency.

It thus can be summed up that there is no theory available presently to simulate the bubble formation and detachment with all the influencing factors. Great effort has to be devoted to seek theories explain more on bubble formation process.

THEORETICAL ANALYSIS

The processes governing the growth and detachment of vapour bubbles formed in liquid are determined mainly by the interactions resulting from the hydrodynamic behaviour of the bubbles with surrounding liquid and by the temperatures field of the liquid around the bubble. In order to evaluate the interaction between bubbles and the liquid phase, the flow field around the bubbles is always required. Furthermore, to establish the growth of the vapour bubble the heat transfer between the liquid and vapour is required, necessitating the calculation of the temperature field.

In this paper, on the basis of potential theory, the equations of motion and the associated pressure field are derived for spherical bubbles growing from a two orifices on a horizontal plate in an assumed inviscid and irrotational liquid. The velocity fields determined from the potential functions are used in the thermal energy equation, which is solved numerically by the finite-difference technique.

To arrive conveniently at a set of generally applicable equations describing bubble motion and the temperature distribution, various simplifications have to be introduced. The

first approximation made is that the bubble is spherical throughout formation and its motion is not affected by the preceding bubble. The second approximation is to assume that the effect of viscosity may be ignored because for liquids such as water the magnitudes of viscous stresses are very much less than those of inertial forces due to liquid motion around the accelerating growing bubble. Also, since the bubble growth rate is very small compared with the velocity of sound in the liquid, compressibility effects may be neglected. The rapid circulation of vapour in the bubble and the large thermal diffusivity of vapour make the temperature and pressure in the bubble uniform. In this study, a constant vapour flow rate through the orifices is adopted.

Two expanding spherical bubbles moving at right angles to the line of centres in the presence of plane wall

Consider two expanding spheres, centres A, B and radii a, b , move with velocities U, V parallel in direction and at right angles to AB ; Figure (1). The expansion rates of the spheres A and B are given by \dot{a} and \dot{b} respectively.

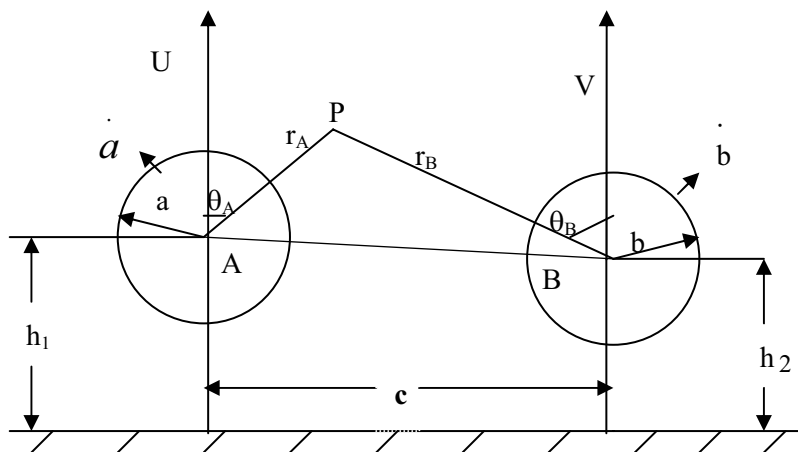


Figure 1: two expanding spheres moving at right angles to the line of centers above a horizontal wall.

The motion of the surrounding liquid due to the spheres is assumed to be irrotational and described by a harmonic velocity potential ϕ . The velocity potential ϕ will be of the form:

$$\phi = \phi_A + \phi_B \tag{1}$$

Where ϕ_A and ϕ_B are the potential velocity of the fluid due to the spheres A and B , respectively and both ϕ_A & ϕ_B satisfy the Laplace equation throughout the fluid:

$$\Delta^2 \phi_A = \Delta^2 \phi_B = 0$$

Subject to the boundary conditions:

$$-\left(\frac{\partial \phi_A}{\partial r_A}\right)_{r_A=a} = \dot{a} + U \cos \theta_A \quad (2.a)$$

$$-\left(\frac{\partial \phi_B}{\partial r_B}\right)_{r_B=b} = \dot{b} + V \cos \theta_B \quad (2.b)$$

$$-\left(\frac{\partial \phi_A}{\partial r_B}\right)_{r_B=b} = 0 \quad (2.c)$$

$$-\left(\frac{\partial \phi_B}{\partial r_A}\right)_{r_A=a} = 0 \quad (2.d)$$

If the distance c between the spheres centres is very great, each sphere will be almost unaffected by the presence of the other, and we shall have, as a first approximation to the potential velocity of the fluid ϕ_A due to the growth spherical bubble above a horizontal plane derived in previous work of Arebi & Dempster [3] as:

$$\begin{aligned} \phi_A = & U \left[\frac{a^3}{2r_A^2} + \frac{a^3 r_A}{8h_1^3} + \frac{a^6}{16h_1^3 r_A^2} + \frac{a^6 r_A}{64h_1^6} + \dots \right] \cos \theta_A + \\ & + \dot{a} \left[\frac{a^2}{r_A} - \left(\frac{a^2 r_A}{4h_1^2} + \frac{a^5}{8h_1^2 r^2} + \frac{a^5 r_A}{32h_1^5} + \dots \right) \cos \theta_A \right] + \\ & + U \left[\frac{3a^3 r_A^2}{64h_1^4} - \frac{a^3}{8h_1^2} - \frac{a^6}{64h_1^5} + \frac{3a^6 r_A^2}{512h_1^7} + \frac{3a^8}{96h_1^4 r_A^3} + \dots \right] + \\ & + \dot{a} \left[\frac{a^2}{2h_1} - \frac{a^2 r_A^2}{16h_1^3} + \frac{a^5}{32h_1^4} - \frac{3a^5 r_A^2}{256h_1^6} - \frac{a^7}{24h_1^3 r_A^3} + \dots \right] + \\ & - U \left[\frac{9a^3 r_A^2}{64h_1^4} + \frac{9a^6 r_A^2}{512h_1^7} + \frac{9a^8}{96h_1^4 r_A^3} + \dots \right] \cos^2 \theta_A + \\ & + \dot{a} \left[\frac{9a^5 r_A^2}{256h_1^6} + \frac{a^7}{8h_1^3 r_A^3} + \frac{3a^2 r_A^2}{16h_1^3} + \dots \right] \cos^2 \theta_A \end{aligned} \quad (3)$$

Let the position of an arbitrary point P be fixed in a meridian plane by its polar coordinates (r_A, θ_A) referred to A and (r_B, θ_B) referred to B; Figure (1). For moderate distance c between the two centres of the spheres at a point in the fluid near B, we shall have: $r_A \cos \theta_A = r_B \cos \theta_B$ and $r_A = (c / \sin \theta_A) - r_B (\sin \theta_B / \sin \theta_A)$.

Now when c is large compared to the radius of the spheres (A & B), at point near B is $r_A \cong c$, therefore; from equation (3) by substituting the above approximation, then:

$$\begin{aligned}
\varnothing_A = & U \left[\frac{a^3 r_B}{2c^3} + \frac{a^3 r_B}{8h_1^3} + \frac{a^6 r_B}{16h_1^3 c^3} + \frac{a^6 r_B}{64h_1^6} \right] \cos \theta_B + \\
& + \dot{a} \left[\frac{a^2}{c} - \left(\frac{a^2 r_B}{4h_1^2} + \frac{a^5 r_B}{8h_1^2 c^3} + \frac{a^5 r_B}{32h_1^5} + \dots \right) \cos \theta_B \right] + \\
& + U \left[\frac{3a^3 c^2}{64h_1^4} - \frac{a^3}{8h_1^2} - \frac{a^6}{64h_1^5} + \frac{3a^6 c^2}{512h_1^7} + \frac{3a^8}{96h_1^4 c^3} + \dots \right] + \\
& + \dot{a} \left[\frac{a^2}{2h_1} - \frac{a^2 c^2}{16h_1^3} + \frac{a^5}{32h_1^4} - \frac{3a^5 c^2}{256h_1^6} - \frac{a^7}{24h_1^3 c^3} + \dots \right] + \\
& - U \left[\frac{9a^3 r_B^2}{64h_1^4} + \frac{9a^6 r_B^2}{512h_1^7} + \frac{9a^8 r_B^2}{96h_1^4 c^5} + \dots \right] \cos^2 \theta_B + \\
& + \dot{a} \left[\frac{9a^5 r_B^2}{256h_1^6} + \frac{a^7 r_B^2}{8h_1^3 c^5} + \frac{3a^2 r_B^2}{16h_1^3} + \dots \right] \cos^2 \theta_B
\end{aligned} \tag{4}$$

This gives over sphere B the normal velocity:

$$\begin{aligned}
-\left(\frac{\partial \varnothing_A}{\partial r_B} \right)_{r_B=b} = & -U \left[\frac{a^3}{2c^3} + \frac{a^3}{8h_1^3} + \frac{a^6}{16h_1^3 c^3} + \frac{a^6}{64h_1^6} \right] \cos \theta_B \\
& - \dot{a} \left[- \left(\frac{a^2}{4h_1^2} + \frac{a^5}{8h_1^2 c^3} + \frac{a^5}{32h_1^5} \right) \cos \theta_B \right] + \\
& + U \left[\frac{9a^3 b}{32h_1^4} + \frac{9a^6 b}{256h_1^7} + \frac{9a^8 b}{48h_1^4 c^5} \right] \cos^2 \theta_B \\
& - \dot{a} \left[\frac{9a^5 b}{128h_1^6} + \frac{a^7 b}{4h_1^3 c^5} + \frac{3a^2 b}{8h_1^3} \right] \cos^2 \theta_B
\end{aligned} \tag{5}$$

This causes the boundary condition (2.c) to be violated; then, this velocity can be cancelled by adding the following terms to the right hand side of equation (4):

$$\begin{aligned}
U \left[\frac{a^3 b^3}{4c^3 r_B^2} + \frac{a^3 b^3}{16h_1^3 r_B^2} + \frac{a^6 b^3}{32h_1^3 c^3 r_B^2} + \frac{a^6 b^3}{128h_1^6 r_B^2} \right] \cos \theta_B + \\
- \dot{a} \left[\frac{a^2 b^3}{8h_1^2 r_B^2} + \frac{a^5 b^3}{16h_1^2 c^3 r_B^2} + \frac{a^5 b^3}{64h_1^5 r_B^2} \right] \cos \theta_B + \\
- U \left[\frac{3a^3 b^5}{32h_1^4 r_B^3} + \frac{3a^6 b^5}{256h_1^7 r_B^3} + \frac{3a^8 b^5}{48h_1^4 c^5 r_B^3} \right] \cos^2 \theta_B + \\
+ \dot{a} \left[\frac{3a^5 b^5}{128h_1^6 r_B^3} + \frac{a^7 b^5}{12h_1^3 c^5 r_B^3} + \frac{a^2 b^5}{8h_1^3 r_B^3} \right] \cos^2 \theta_B
\end{aligned} \tag{6}$$

This Leading to an approximate expression for \varnothing_A in the presence of B as: (equation 3 + equation 6). Similarly, the corresponding approximate expression for \varnothing_B may be found with same procedure adopted in case of sphere A.

The approximate expression for \varnothing_A gives over A an excessive normal velocity which can be cancelled again by adding suitable terms of higher order to the approximate

expression for \varnothing_A (equation 3 + equation 6), which is give order of approximation may be acceptable however since $c \gg \max(a,b)$. The potential velocity will be of the form: $\varnothing = \varnothing_A + \varnothing_B$.

Near sphere A, since $r_B \cos \theta_B = r_A \cos \theta_A$ and $r_B \approx c$; Figure (1), we have:

$$\varnothing(\text{near A}) = E + G + I + K$$

Where:

$$\begin{aligned}
 E = & U \left[\frac{a^3}{2 r_A^2} + \frac{a^3 r_A}{8 h_1^3} + \frac{a^6}{16 h_1^3 r_A^2} + \frac{a^6 r_A}{64 h_1^6} + \dots \right] \cos \theta_A + \\
 & + \dot{a} \left[\frac{a^2}{r_A} - \left(\frac{a^2 r_A}{4 h_1^2} + \frac{a^5}{8 h_1^2 r_A^2} + \frac{a^5 r_A}{32 h_1^5} + \dots \right) \cos \theta_A \right] + \\
 & + U \left[\frac{3 a^3 r_A^2}{64 h_1^4} - \frac{a^3}{8 h_1^2} - \frac{a^6}{64 h_1^5} + \frac{3 a^6 r_A^2}{512 h_1^7} + \frac{3 a^8}{96 h_1^4 r_A^3} + \dots \right] + \\
 & + \dot{a} \left[\frac{a^2}{2 h_1} - \frac{a^2 r_A^2}{16 h_1^3} + \frac{a^5}{32 h_1^4} - \frac{3 a^5 r_A^2}{256 h_1^6} - \frac{a^7}{24 h_1^3 r_A^3} + \dots \right] + \\
 & - U \left[\frac{9 a^3 r_A^2}{64 h_1^4} + \frac{9 a^6 r_A^2}{512 h_1^7} + \frac{9 a^8}{96 h_1^4 r_A^3} + \dots \right] \cos^2 \theta_A + \\
 & + \dot{a} \left[\frac{9 a^5 r_A^2}{256 h_1^6} + \frac{a^7}{8 h_1^3 r_A^3} + \frac{3 a^2 r_A^2}{16 h_1^3} + \dots \right] \cos^2 \theta_A + \\
 & + U \left[\frac{a^3 b^3 r_A}{4 c^6} + \frac{a^3 b^3 r_A}{16 h_1^3 c^3} + \frac{a^6 b^3 r_A}{32 h_1^3 c^6} + \frac{a^6 b^3 r_A}{128 h_1^6 c^3} \right] \cos \theta_A \\
 \\
 G = & - \dot{a} \left[\frac{a^2 b^3 r_A}{8 h_1^2 c^3} + \frac{a^5 b^3 r_A}{16 h_1^2 c^6} + \frac{a^5 b^3 r_A}{64 h_1^5 c^3} + \dots \right] \cos \theta_A + \\
 & - U \left[\frac{3 a^3 b^5 r_A^2}{32 h_1^4 c^5} + \frac{3 a^6 b^5 r_A^2}{256 h_1^7 c^5} + \frac{3 a^8 b^5 r_A^2}{48 h_1^4 c^{10}} + \dots \right] \cos^2 \theta_A + \\
 & + \dot{a} \left[\frac{3 a^5 b^5 r_A^2}{128 h_1^6 c^5} + \frac{a^7 b^5 r_A^2}{12 h_1^3 c^{10}} + \frac{a^2 b^5 r_A^2}{8 h_1^3 c^5} + \dots \right] \cos^2 \theta_A \\
 & + V \left[\frac{b^3 r_A}{2 c^3} + \frac{b^3 r_A}{8 h_2^3} + \frac{a^6 r_A}{64 h_2^6} + \dots \right] \cos \theta_A + \\
 & + \dot{b} \left[\frac{b^2}{c} - \left(\frac{b^2 r_A}{4 h_2^2} + \frac{b^5 r_A}{8 h_2^2 c^3} + \frac{b^5 r_A}{32 h_2^5} + \dots \right) \cos \theta_A \right]
 \end{aligned}$$

$$\begin{aligned}
I = & V \left[\frac{3b^3 c^2}{64h_2^4} - \frac{b^3}{8h_2^2} - \frac{b^6}{64h_2^5} + \frac{3b^6 c^2}{512h_2^7} + \frac{3b^8}{96h_2^4 c^3} + \dots \right] + \\
& + \dot{b} \left[\frac{b^2}{2h_2} - \frac{b^2 c^2}{16h_2^3} + \frac{b^5}{32h_2^4} - \frac{3b^5 c^2}{256h_2^6} - \frac{b^7}{24h_2^3 c^3} + \dots \right] + \\
& - V \left[\frac{9b^3 r_A^2}{64h_2^4} + \frac{9a^6 r_A^2}{512h_2^7} + \frac{9b^8 r_A^2}{96h_2^4 c^3} + \dots \right] \cos^2 \theta_A + \\
& + \dot{b} \left[\frac{9b^5 r_A^2}{256h_2^6} + \frac{b^7 r_A^2}{8h_2^3 c^3} + \frac{3b^2 r_A^2}{16h_2^3} + \dots \right] \cos^2 \theta_A + \\
& + V \left[\frac{b^3 a^3}{4c^3 r_A^2} + \frac{b^3 a^3}{16h_2^3 r_A^2} + \frac{b^6 a^3}{32h_2^3 c^3 r_A^2} + \frac{b^6 a^3}{128h_2^6 r_A^2} \right] \cos \theta_A \\
K = & -\dot{b} \left[\frac{b^2 a^3}{8h_2^2 r_A^2} + \frac{b^5 a^3}{16h_2^2 c^3 r_A^2} + \frac{b^5 a^3}{64h_2^5 r_A^2} + \dots \right] \cos \theta_A + \\
& - V \left[\frac{3b^3 a^5}{32h_2^4 r_A^3} + \frac{3b^6 a^5}{256h_2^7 r_A^3} + \frac{3b^8 a^5}{48h_2^4 c^3 r_A^3} + \dots \right] \cos^2 \theta_A + \\
& + \dot{b} \left[\frac{3b^5 a^5}{128h_2^6 r_A^3} + \frac{b^7 a^5}{12h_2^3 c^3 r_A^3} + \frac{b^2 a^5}{8h_2^3 r_A^3} + \dots \right] \cos^2 \theta_A \tag{7}
\end{aligned}$$

Thus $\phi_{nearA} = f(U, V, \dot{a}, \dot{b}, a, b, r_A, \theta_A, c, h_1, h_2)$

Special Cases

Equation (7) is the general equation of two expanding spheres (or bubbles) moving at right angles to the line of centres in the presence of a horizontal plane. The following special cases are obtainable:

- (1) By setting $h_1 \rightarrow \infty$ and $h_2 \rightarrow \infty$ in equation (7) we get the velocity potential due to the two expanding spheres moving at right angles to the line of centers in the absence of any nearby surface.
- (2) By setting $h_2 \rightarrow \infty$ and $c \rightarrow \infty$ in equation (7) we get the velocity potential due to the one expanding sphere moving above a horizontal plane.
- (3) By setting $h_2 \rightarrow \infty, h_1 \rightarrow \infty$ and $c \rightarrow \infty$ in equation (7) we have the velocity potential due to the one expanding sphere moving in the absence of any nearby surface.

Equation of motion

For a gas or vapour bubble growing at an orifice in an inviscid liquid, the forces acting on the bubble result from the following:

- (1) surface tension force, F_s acting around the rim of the orifice, is given by:

$$F_s = \pi d_o \zeta \sin \alpha$$

where d_o = the orifice diameter, ζ = surface tension coefficient, α = the bubble bottom contact angle, because of lack of information on α , α is taken to be 90° , the surface tension force is in the downward direction.

- (2) Gas (or vapour) momentum force: the gas (or vapour) momentum has a significant effect on the bubble growth at high system pressure and high injection velocity, the contribution of its force F_m which acts upwards, is taken into account and given by:

$$F_m = \frac{4 \rho_g q_s^2}{\pi d_o^2}$$

Where q_s = the volumetric flow rate of the gas (or vapour), m^3/sec , ρ_g = gas or vapour density kg/m^3 .

- (3) Liquid phase pressure: the force on the bubble due to the fluid pressure P is:

$$F_P = 2\pi a^2 \int_0^\pi (P \sin \theta \cos \theta) d\theta$$

According to Bernoulli's theorem, the liquid pressure is given by:

$$\frac{P}{\rho_L} + \frac{1}{2} q^2 - \frac{\partial \phi}{\partial t} - g(x) = constant$$

where q is the absolute liquid velocity and ρ_L is the liquid density.

From the Bernoulli's equation, the pressure force can be divided into two kinds: (i) liquid inertia force; (ii) the force due to static pressure from the $g(x)$ term. If F_i is the liquid inertia force in the downward direction, then:

$$F_i = 2\pi a^2 \rho_L \int_0^\pi \left(\frac{\partial \phi}{\partial t} - \frac{1}{2} q^2 \right) \sin \theta \cos \theta d\theta \quad (8)$$

$$where \quad q = \sqrt{\left(\frac{\partial \phi}{\partial r} \right)^2 + \left(\frac{1}{r} \frac{\partial \phi}{\partial \theta} \right)^2} \quad (9)$$

The force due to static pressure is represented by the buoyancy force F_B which acts in an upwards direction. If the mass of steam is included, the buoyancy force F_B is:

$$F_B = \frac{4\pi}{3} a^3 g (\rho_L - \rho_g)$$

The potential velocity ϕ equation (7), may now be used to find the liquid inertia force for the case of two bubbles growing at two neighboring orifices by putting the potential velocity of equation (7) in equation (9) and then equation (9) where the time derivative of ϕ is equal to;

$$\begin{aligned} & \frac{\partial \phi}{\partial r} \frac{dr}{dt} + \frac{\partial \phi}{\partial \theta} \frac{d\theta}{dt} + \frac{\partial \phi}{\partial a} \frac{da}{dt} + \frac{\partial \phi}{\partial h_1} \frac{dh_1}{dt} + \frac{\partial \phi}{\partial b} \frac{db}{dt} + \frac{\partial \phi}{\partial h_2} \frac{dh_2}{dt} + \\ & \frac{\partial \phi}{\partial U} \frac{dU}{dt} + \frac{\partial \phi}{\partial V} \frac{dV}{dt} + \frac{\partial \phi}{\partial \dot{a}} \frac{d\dot{a}}{dt} + \frac{\partial \phi}{\partial \dot{b}} \frac{d\dot{b}}{dt} + \frac{\partial \phi}{\partial c} \frac{dc}{dt} \end{aligned}$$

The origin of the co-ordinates system is in motion, and the values of r and θ for a fixed point P in space are therefore increasing at the rates:

$$\frac{dr}{dt} = -U \cos \theta, \quad \frac{d\theta}{dt} = \frac{U}{r} \sin \theta \quad \text{and} \quad U = \frac{dh}{dt}$$

Since the bubbles are moving at right angles to the line of centres, the change of the distance, c between the centres of the two bubbles A, B during the formation of the bubbles is very small in comparison with the distance c . Therefore, it is assumed that $\frac{dc}{dt} = 0$.

Also the centre of the bubble cannot be closer to the plane wall than its radius ($h \geq a$) and $c > \max(a, b)$ therefore the term of $\left((a^J b^k C^{m-1}) / (h_1^N h_2^x c^{y-1}) \right)$ may be neglected where $\{(J+k+m) \leq (N+x+y) \geq 7\}$.

Substituting for q and \emptyset in equation (9) and then in equation (8); (note that we are interested in conditions near the surface of the bubble ($r \cong a$)). The result equation is:

$$\begin{aligned} F_i = 2\pi a^2 \rho_{liq} & \left[\ddot{h}_1 \left(\frac{a}{3} + \frac{a^4}{8h_1^3} + \frac{a^7}{96h_1^6} \right) - \ddot{a} \left(\frac{a^3}{4h_1^2} + \frac{a^6}{48h_1^5} + \frac{a^3 b^3}{12h_1^2 c^3} \right) + \right. \\ & + \ddot{h}_2 \left(\frac{b^3 a}{2c^3} + \frac{b^3 a}{8h_2^3} + \frac{a^7}{96h_2^6} + \frac{b^6 a}{192h_2^6} \right) - \ddot{b} \left(\frac{b^2 a}{4h_2^2} + \frac{b^5 a}{8h_2^2 c^3} + \frac{b^5 a}{32h_2^5} \right) + \\ & + \dot{a} \dot{h} \left(1 + \frac{3a^3}{4h_1^3} + \frac{29a^6}{480h_1^6} \right) - \dot{a}^2 \left(\frac{3a^2}{4h_1^2} + \frac{a^5}{24h_1^5} + \frac{a^3 b^3}{6h_1^3 c^3} \right) + \\ & + \dot{a} \dot{h}_2 \left(\frac{b^3}{8h_2^3} + \frac{b^3}{2c^3} + \frac{b^6}{64h_2^6} - \frac{3b^3 a^3}{64h_1^2 h_2^4} - \frac{b^3 a^3}{32h_1^3 h_2^3} \right) + \\ & - \dot{a} \dot{b} \left(\frac{b^2}{4h_2^2} + \frac{b^5}{8h_2^2 c^3} + \frac{b^5}{32h_2^5} + \frac{b^2 a^3}{4h_1^2 c^3} - \frac{b^2 a^3}{16h_1^2 h_2^3} - \frac{b^2 a^3}{16h_1^3 h_2^2} \right) + \\ & + \dot{b} \dot{h}_2 \left(\frac{3b^2 a}{2c^3} + \frac{7b^2 a}{8h_2^3} + \frac{25.5b^5 a}{96h_2^6} \right) + \\ & \left. - \dot{b}^2 \left(\frac{ba}{2h_2^2} + \frac{5b^4 a}{8h_2^2 c^3} + \frac{3b^4 a}{32h_2^5} \right) - \dot{h}_1^2 \left(\frac{3a^4}{16h_1^4} \right) - \dot{h}_2^2 \left(\frac{3b^3 a}{8h_2^4} \right) \right] \end{aligned} \quad (10)$$

$$\text{where } \dot{h} = \frac{dh}{dt}, \quad \ddot{h} = \frac{d^2 h}{dt^2}, \quad \ddot{a} = \frac{d^2 a}{dt^2} \quad \text{and} \quad \dot{a} = \frac{da}{dt}$$

The total force F_t acting on the bubble in the upward direction is:

$$F_t = F_B + F_m - F_s - F_i$$

The required equation of motion for the bubble in the upward direction may then be written as:

$$\frac{d}{dt} \left(\frac{4\pi}{3} a^3 \rho_s \dot{h} \right) = F_t, \quad F_t > 0$$

The surface tension force F_s and the momentum force are assumed to be constant due to their definition; the two governing forces at the detachment time are the buoyancy and the inertia forces. The buoyancy force F_B increases continually as the bubble volume increases. As the expansion velocity is very high at the beginning, the inertia force is great initially, and then decreases sharply due to the large reduction in the growth velocity. When the net force is positive, the bubble as a whole accelerates and the inertia force increases gradually until at a certain point of time, the net force is negative again. When the net force on the bubble becomes negative the movement of the bubble is decelerated and may stop instantaneous, since its momentum has been neglected, at this point the movement of the bubble centre is again caused only by the expansion of the bubble, and therefore the inertia force drops to the level of the inertia force caused by the expansion of the bubble only.

Thermal equation (energy equation)

The liquid temperature field is considered to be axis-metrical around the bubble. In spherical coordinates, the partial differential thermal energy equation has the form:

$$\frac{\partial T}{\partial t} + U_r \frac{\partial T}{\partial r} + \frac{U_\theta}{r} \frac{\partial T}{\partial \theta} = \alpha \left(\frac{\partial^2 T}{\partial r^2} + \frac{2}{r} \frac{\partial T}{\partial r} + \frac{\cos \theta}{r^2 \sin \theta} \frac{\partial T}{\partial \theta} + \frac{1}{r^2} \frac{\partial^2 T}{\partial \theta^2} \right) \quad (11)$$

Where α is the thermal diffusivity, θ is the angle measured from bubble top, $U_r = -\frac{\partial \phi}{\partial r}$ is the radial velocity, $U_\theta = -\frac{1}{r} \frac{\partial \phi}{\partial \theta}$ is the tangential velocity.

Since the thermal diffusivity of the water is small, the thermal boundary layer around the bubble is assumed to be thin. In the numerical analysis, the thickness of the thermal boundary layer is assumed to be a distance of half the bubble radius away from the bubble surface. The numerical solutions confirm the thin thermal boundary layer assumption.

Equation (11) is solved numerically by the five-point method of the finite difference technique. Also the numerical results show that the molecular conduction in the direction tangential to the bubble surface is negligible compared with the convective transport in that direction, and the contribution to radial conduction from the first order radial term will be small compared with that of the second order term and can be ignored. Thus, equation (11) may be approximated by:

$$\frac{\partial T}{\partial t} + U_r \frac{\partial T}{\partial r} + \frac{U_\theta}{r} \frac{dT}{d\theta} = \alpha \frac{\partial^2 T}{\partial r^2} \quad (12)$$

Since the thermal diffusivity of the vapour is large, the temperature gradients within the bubble are negligible, and the interior of the bubble is assumed uniform at the saturation temperature, T_s , the temperature at the bubble surface is the steam temperature, T_s of

bubble interior, the wall temperature at the chamber bottom is constant and assumed to be equal to T_∞ ; the liquid temperature at a significant distance from the bubble.

Mass balance equation

Taking the bubble surface contour as the boundary of a control volume, hence, for constant mass flow rate, \dot{m} , the total mass balance for the steam in the bubble is:

$$\frac{\partial(\rho_v V)}{\partial t} = \dot{m} - A_s \dot{m}''$$

$$\text{where } A_s \dot{m}'' = \frac{2\pi R^2 k}{L} \int_0^\pi \left(\frac{\partial T}{\partial r}\right) \sin \theta d\theta$$

If ρ_v is constant, the volume increase rate, $\frac{dV}{dt}$ is given as:

$$\frac{dV}{dt} = q - \frac{2\pi R^2 k}{\rho_v L} \int_0^\pi \left(\frac{\partial T}{\partial r}\right) \sin \theta d\theta$$

$$\text{where } q = \dot{m} / \rho_v \text{ and } R = \left(\frac{3V}{4\pi}\right)^{\frac{1}{3}}$$

where q is the volumetric flow rate (m^3/sec), ρ_v is the steam density (kg/m^3), V is the bubble volume (m^3), \dot{m}'' is the condensing mass flux through the bubble surface ($\text{kg}/\text{m}^2\text{s}$), A_s is the bubble surface area (m^2), L is the specific latent heat of condensation (kJ/kg), k is the water thermal conductivity (kW/mK), R is the bubble radius (m), \dot{m} is the mass flow rate through the orifice (kg/s).

Bubble detachment

Assuming the surface tension force F_s and the steam momentum force F_m are constant, and then the liquid inertial force and the buoyancy force would decide the bubble's detachment. The detachment of the bubble takes place in two stages. During the first stage the total force acts downwards causing a reaction on the surface of the plate, since the bubble is in direct contact with the orifice plate. The assumption of a spherical bubble shape makes the vertical distance of the centre of the bubble (h) equal to the bubble radius (a). This stage terminates when the downward forces on the bubble become equal to the upwards forces. The termination of this stage is referred to as "beginning of detachment". The second stage starts when the growing bubble begins to move away from the orifice plate due to the positive upwards net force but it is still connected to the orifice by a neck. As a result of the positive net upward force, the vertical motion of the bubble is a combination of the motion due to expansion and the motion of the bubble as a whole, which leads to increasing the translation acceleration.

During the secondary growth phase, the magnitude of acceleration due to expansion reduces as the bubble gets bigger; the positive downward force leads to deceleration of bubble motion. This deceleration leads to a reduction in the reacting force from the liquid than before and the total force becomes positive again in the upwards direction, causing the bubble as a whole to accelerate again and so on. This oscillation can be occurred several times depending mainly on the flow rate and sub-cooling temperature. This stage is

referred to as the "elongation stage". The condition for detachment can be described as follows:

$$\Sigma F > 0 \text{ and } \Sigma \dot{F} > 0$$

Numerical procedure

Transform the thermal energy equation into finite difference form as following:

$$\frac{\partial T}{\partial r} = \frac{T_{i+1,j}^k - T_{i,j}^k}{h_2}$$

$$\frac{\partial T}{\partial t} = \frac{T_{i,j}^{k+1} - T_{i,j}^k}{\tau}$$

$$\frac{\partial T}{\partial \theta} = \frac{T_{i,j+1}^k - T_{i,j}^k}{\lambda_2}$$

$$\frac{\partial^2 T}{\partial r^2} = \frac{h_1 T_{i+1,j}^k - (h_1 + h_2) T_{i,j}^k + h_2 T_{i-1,j}^k}{h_1 h_2^2}$$

$$\frac{\partial^2 T}{\partial \theta^2} = \frac{\lambda_1 T_{i,j+1}^k - (\lambda_1 + \lambda_2) T_{i,j}^k + \lambda_2 T_{i,j-1}^k}{\lambda_1 \lambda_2^2}$$

where τ is the time step, (h_1, h_2) are the thicknesses of the two adjacent layers and (λ_1, λ_2) are the two angle segments to the point (i, j) in the same layer.

The thermal energy equation (12) becomes:

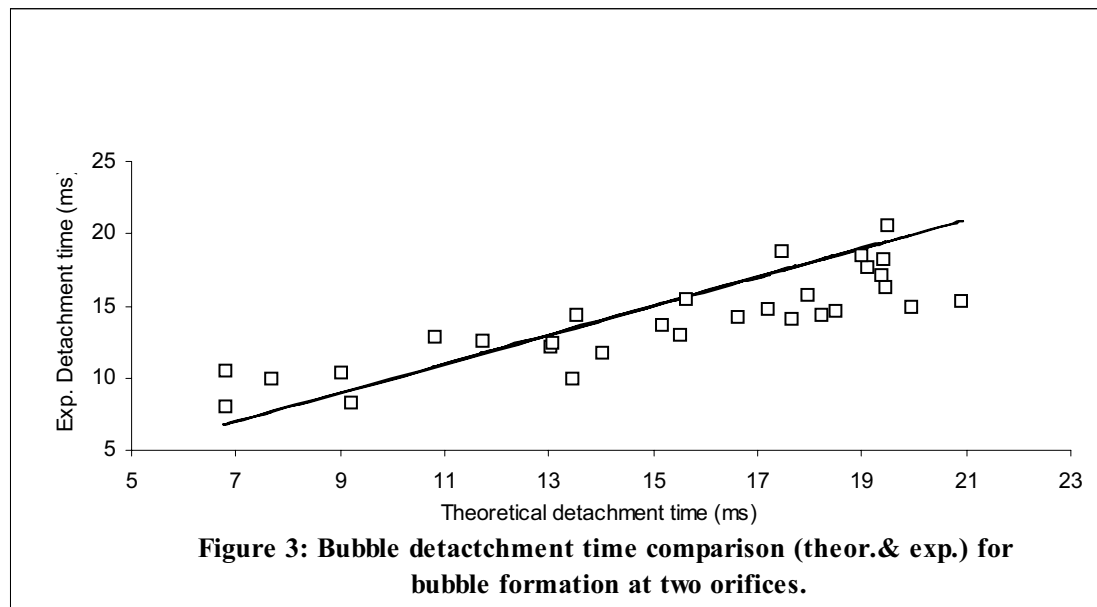
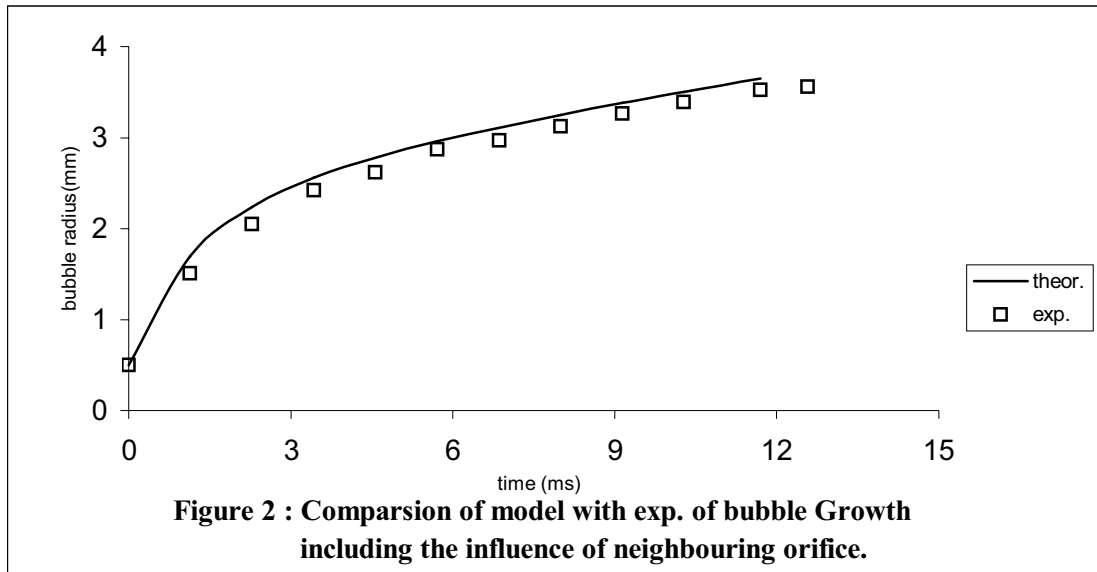
$$T_{i,j}^{k+1} = \frac{\tau}{h_2} \left[\frac{\alpha}{h_2} + \frac{2\alpha}{r} - U \right] T_{i+1,j}^k + \left[\frac{U}{h_2} + \frac{V}{r \lambda_2} + \frac{1}{\tau} - \alpha \frac{h_1 + h_2}{h_1 h_2^2} \right. \\ \left. - \frac{2\alpha}{r h_2} - \frac{\alpha}{r^2 \lambda_2} \text{Cot } \theta - \frac{\alpha}{r^2} \frac{\lambda_1 + \lambda_2}{\lambda_1 \lambda_2^2} \right] \tau T_{i,j}^k + \frac{\alpha \tau}{h_1 h_2} T_{i-1,j}^k \\ + \frac{\tau}{r \lambda_2} \left[\frac{\alpha}{r} \text{Cot } \theta + \frac{\alpha}{r \lambda_2} - V \right] T_{i,j+1}^k + \frac{\alpha}{r^2} \frac{1}{\lambda_1 \lambda_2} T_{i,j-1}^k$$

The initial conditions are:

$$T_{i,j}^0 = T_\infty, \left\{ \begin{array}{l} i = 1, 2, 3, \dots \\ j = 1, 2, 3, \dots \end{array} \right\}$$

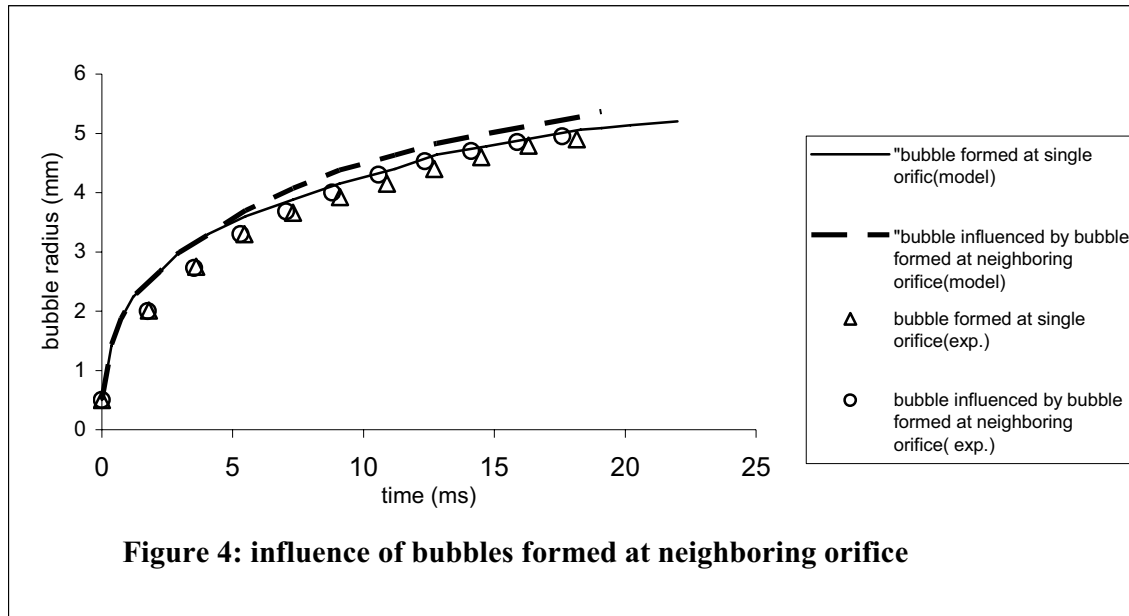
RESULTS AND DISCUSSION

A number of tests have been selected from reference [2] to validate the theoretical model and to study the effect of bubbles formed at neighboring orifices. The comparison between samples of the theoretical curves and the experimental data are shown in Figure (2) and Figure (3). The plots indicate that the theory and experimental results show good agreement.



Steam bubble growth rate

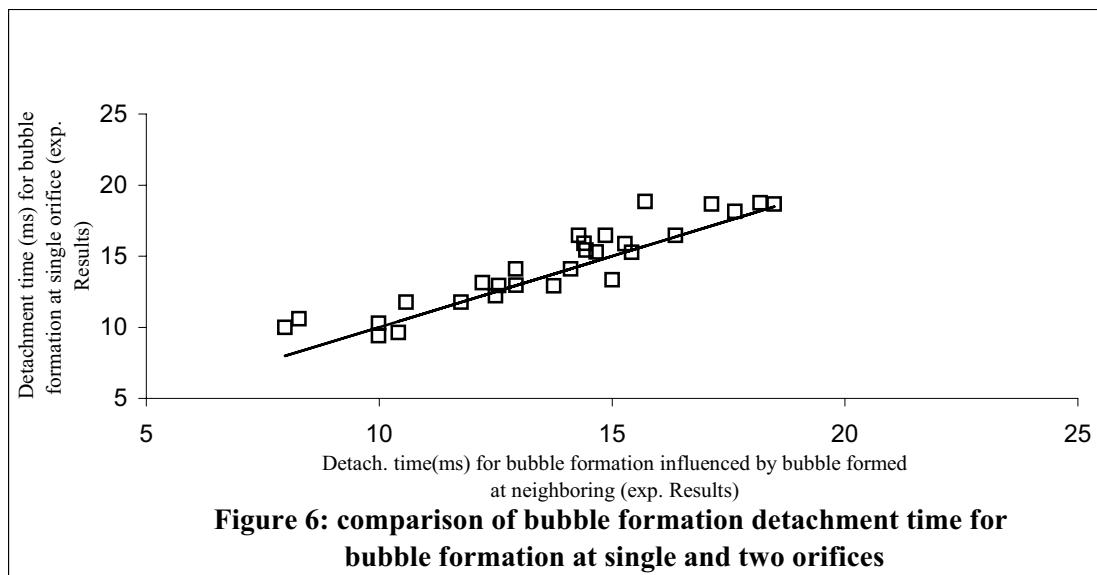
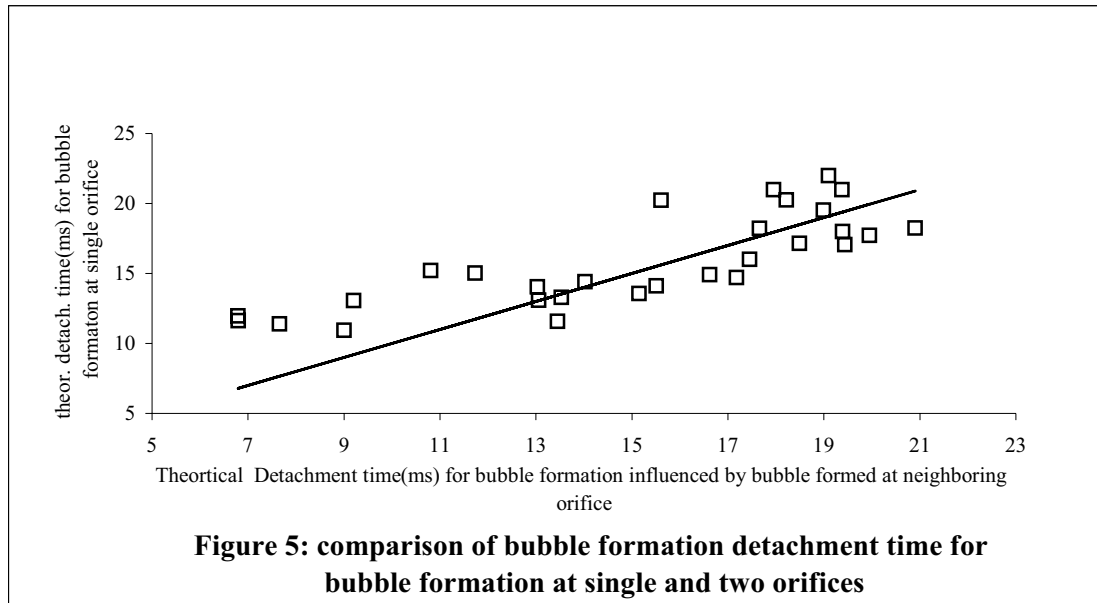
The theoretical and the experimental results (refer to Figure 4) show there is a small effect on the bubble growth due to the bubbles growing at neighbouring orifices. This effect slightly increases the growth rate at the later stage of bubble formation. As the bubble at neighbouring orifice gets bigger, the potential velocity is more influenced and the outer surfaces of the bubbles come close to each other and of possibility that the thermal boundary layers interfere exist.



There are still other factors influencing the rate of bubble growth. In the theory, the influence of preceding collapsing bubbles on the bubble growing at the orifice is not included and the initial temperature field around the bubble is assumed uniform with the value of T_{∞} . However, the preceding bubbles will leave a non uniform temperature $T \geq T_{\infty}$. Moreover, the temperature boundary condition at the wall is made equal to T_{∞} , whereas in the real case, the temperature at the wall will be somewhat greater than T_{∞} as the bubble formation proceeds, thus the theory is expected to predict lower rates of bubble growth, on the other hand; the theoretical study assumes a spherical bubble shape, which is different from experimental observations, especially when the bubble is severely elongated, then the theoretical bubble gives a smaller surface area than that of the real bubble for a given bubble volume. A smaller surface area leads to lower rates of steam condensation. Therefore, the assumption of a spherical bubble predicts lower rates of steam condensation and leads to higher growth rates. These two opposing effects lead to minimise the discrepancy between the experimental and the theoretical results of bubble growth rates.

Bubble formation time and formation frequency

Figure (5) and Figure (6) show comparison between the theoretical and the experimental detachment time of bubbles formed at single orifice and that bubbles influenced by bubbles formed at neighboring orifice. It can be deduced from the figures that the bubble formed at neighboring orifice tends to reduce the detachment time which is leads to higher frequency of bubble formation.



CONCLUSIONS

An idealised picture of bubble formation suggests that the growth of the bubble consists of both a radial expansion and a vertical translation. The relative magnitude of these components depends on the interaction of the forces on the bubble. The potential theory developed to model this process predicts well the velocity fields around the growing and rising bubbles until detachment.

The growth and detachment of the bubble from the orifice has been observed to consist of a two stage process whereby the steam expands spherically as a bubble into the sub-cooled liquid. A point is reached when the main volume of the vapour bubble translates upwards. The two stage approach developed to model this process predicts good results compared with experimental.

Although the theory developed does not include the influence of preceding bubbles, which seems to be important from the experimental observation, especially in the case of

coalescence, the theory; within the limited range of orifices and the spacing between the orifices considered, still predicts the bubble growth rate and detachment time compared with experimental results for the case no coalescence involving. Moreover, , in this study the theoretical and the experimental results show that the formation of a bubble at one orifice would have small effect on the growing bubble at neighboring orifice., the bubble forming at neighboring orifice has been found to slightly increase the bubble volume. The bubble formation time (detachment time) is subject to change and is determined by the interaction of all the forces acting on the bubble where the neighboring bubble tends to reduce the detachment time.

REFERENCES

- [1] Rayleigh, L "On the pressure developed in a liquid during the collapse of a spherical Cavity", Phil. Mag, Vol. 34, (1917), pp 94-98
- [2] Dempster W. m. and Arebi B. H. "Experimental characteristics of steam bubble growth at orifices in sub-cooled liquid" Int. Comm.. Heat Mass Transfer, Vol. 28, No. 4, pp 467 -477, 2001.
- [3] Arebi B. and Dempster W. M. "Theoretical model for the growth and detachment of condensing steam bubbles at submerged orifice" Two- phase flow modelling and experimentation, 1999 pp 397-404
- [4] Davidson, J. F., and Schuler, B. O. G., "Bubble formation at an Orifice in an inviscid Liquid", Trans. Instn. Chem. Engrs., Vol. 38, (1960), pp 335-342.
- [5] Simpson, H. C., Bradford, A. M. and Tao, Z. "The formation of steam bubble at an orifice submerged in subcooled water", European Two Phase Flow Group Meeting, Paris, (1989).
- [6] Cho, S. C. and Lee, W. K., "Steam bubble formation at a submerged orifice in quiescent water", Chem. Eng. Sci., Vol. 46, No. 3, (1991), pp 789-795.
- [7] Schmidt, H., "Bubble formation and heat transfer during dispersion of superheated steam in saturated water - I: Bubble size and bubble detachment at single orifices", Int. J. Heat Trans., Vol.20, (1976), pp 635-646.
- [8] Ruzicka M., Drahos J. , Zahrdnik N. , Thomas N. H. "Natural modes of multi-orifice bubbling from a Common Plnum" Chem. Eng. Sci. vol. 54 (1999) pp 5223-5229
- [9] Ruzicka M., Drahos J. , Zahrdnik N. , Thomas N. H. "Structure of gas pressure signal at two orifices bubbling from a common plenum" Chem. Eng. Sci. vol. 55 (2000) pp 421-429.
- [10] Shuki Xie, Reginald H. Tan "Bubble formation at multiple orifices-bubbling synchronicity and frequency" Chem. Eng. Sci. Vol. 58 (2003) pp 4639-4647
- [11] Pereira Dias. M. I. "Bubble formation at multiple orifice plate submerged in quiescent liquid" PhD. thesis, University Libre De Bruxelles and Von Karman Institute for Fluid Dynamics (1999).